Magnetic anisotropy of iron multilayers on Au(001): First-principles calculations in terms of the fully relativistic spin-polarized screened KKR method

L. Szunyogh
Institut für Technische Elektrochemie, Technische Universität Wien, Getreidemarkt 9/158, A-1060, Wien, Austria and Institute of Physics, Technical University Budapest, Budafoki út 8, H-1111, Budapest, Hungary

B. Újfalussy
Institut für Technische Elektrochemie, Technische Universität Wien, Getreidemarkt 9/158, A-1060, Wien, Austria and Research Institute for Solid State Physics, Hungarian Academy of Sciences, H-1525 Budapest, P.O. Box 49, Hungary

P. Weinberger
Institut für Technische Elektrochemie, Technische Universität Wien, Getreidemarkt 9/158, A-1060, Wien, Austria
(Received 4 November 1994; revised manuscript received 13 December 1994)

In order to treat the orientation of the magnetic field at surfaces properly, the spin-polarized fully relativistic version of the screened Korringa-Kohn-Rostoker method for semi-infinite systems is presented. Magnetic anisotropy energies up to six iron layers on Au(001) are calculated by using the force theorem, predicting a change from a perpendicular to a parallel magnetization for a layer thickness between three and four layers of Fe, in very good agreement with experimental observations. In particular, the magnetic anisotropy energy is discussed in relation to the orbital magnetic moment and to the orientation of the magnetic field when changed continuously.

I. INTRODUCTION

Since recently many overlayer and superlattice systems have been predicted to be useful for purposes of high-density magneto-optical storage,[1,2] theoretical investigations of the magnetic anisotropy of such systems became of particular interest. As proposed originally by van Vleck,[3] the magnetic anisotropy arises primarily from a spin-orbit coupling (SOC) interaction. Since, in particular, for 3*d* transition metals, this interaction energy is thought to be fairly small as compared to the 3*d* bandwidth, perturbative treatments of SOC have been applied in many theoretical investigations. Tight-binding studies cleared up some important features of the magnetic anisotropy for monolayers and multilayers, in particular with respect to the orbital moment anisotropy, band-filling, and crystal-field effects.[4–6] Concomitantly, a large variety of *ab initio* calculations within the local spin density approximation (LSDA) and by using the "force theorem" have been published,[7–15] yielding mostly good quantitative explanations or predictions for the magnetic anisotropy of several layered ferromagnetic systems.

However, for systems containing heavy elements it is *a priori* not evident that the SOC can be treated as a perturbation. It seemed therefore desirable to develop techniques based on a nonperturbative treatment of SOC, namely to use a fully relativistic description.[16] Solutions of the Dirac Hamiltonian in the presence of a magnetic field have been discussed by Feder and Rosicky[17] and Strange *et al.*[18] that, in turn, allow a proper description of the orientation of the magnetic field. This approach has then been incorporated to the Korringa-Kohn-Rostoker (KKR) method[19–21] and the linear muffin-tin orbital (LMTO) method.[22,23] The latter technique was used, for example, by Guo *et al.* to compute the magnetic anisotropy energy of a single Fe layer[24] and of thin Fe films[25] in noble metals.

Experimental studies reveal a pseudomorphic epitaxial growth of ultrathin Fe films on a Au(001) 1×1 surface,[26–28] because of a very small misfit between the lattice constant of the 2D fcc(001) lattice of Au and that of the bcc Fe, and because of the Au atoms segregating at the top of the film.[29] Liu and Bader found that when grown at 100 K these films have a magnetization perpendicular to the surface for thicknesses less then 2.8 monolayers (ML) and in-plane magnetization beyond that.[28] In this paper, the spin-polarized relativistic version of the screened KKR method[30] is applied to calculate the magnetic anisotropy energy of the $Fe_nAu(001)$, $n \leq 6$, multilayer systems. Theoretical aspects concerning the relativistic spin-polarization are described in Sec. II. Approximations used in our model are mentioned in Sec. III together with some of the computational details. In Sec. IV the results for the $Fe_nAu(001)$ films are presented and discussed.

II. THEORY

Within the relativistic density functional theory[31,32] and by employing the Gordon decomposition for the current,[33] the Kohn-Sham-Dirac Hamiltonian can be

written as[18]

$$\mathcal{H} = c\boldsymbol{\alpha}\mathbf{p} + \beta mc^2 + I_4 V^{\text{eff}}[n,\mathbf{m}] + \beta\boldsymbol{\sigma}\mathbf{B}^{\text{eff}}[n,\mathbf{m}], \quad (1)$$

where the α_i (i=1,2,3) and β are Dirac matrices, σ_i (i=1,2,3) Pauli matrices, I_4 is a 4×4 unit matrix, and n and $\mathbf{m}$ denote the particle density and the spin magnetization density, respectively. If the effective potential $V^{\text{eff}}[n,\mathbf{m}]$ and the effective magnetic field $\mathbf{B}^{\text{eff}}[n,\mathbf{m}]$ is spherical symmetric and the magnetic field points along the z axis, i.e.,

$$V^{\text{eff}}(\mathbf{r}) = V(r)\,, \quad (2)$$
$$\mathbf{B}^{\text{eff}}(\mathbf{r}) = B(r)\,\hat{\mathbf{z}}\,, \quad (3)$$

Eq. (1) reduces to

$$\mathcal{H} = c\boldsymbol{\alpha}\mathbf{p} + \beta mc^2 + I_4 V(r) + \beta\sigma_z B(r)\,. \quad (4)$$

For a finite-range spherical symmetric potential and magnetic field, the corresponding single-site scattering problem was discussed by Feder and Rosicky[17] and Strange *et al.*,[18] by neglecting the (second order) coupling between scattering channels belonging to different values of the angular momentum quantum number ℓ. This approach, which reduces enormously the numerical effort in solving the corresponding radial Dirac equation, has opened up a way for a study of magnetism on the scale of a relativistic electron theory and will be used also in the present paper. Only very recently, Jenkins and Strange[34] emphasized that keeping the full coupling in the radial Dirac equation might be important in some applications. Also rather recently, the single-site scattering problem was discussed for a space-filling full potential by Lovatt *et al.*[35]

For the purpose of magnetic anisotropy calculations it is essential to determine the single-site $\mathbf{t}$ matrix corresponding to different orientations of the magnetic field. Such an arbitrary situation is shown in Fig. 1. Let $R = R(\Theta,\phi) \in \mathrm{O}(3)$ be the rotation, which transforms

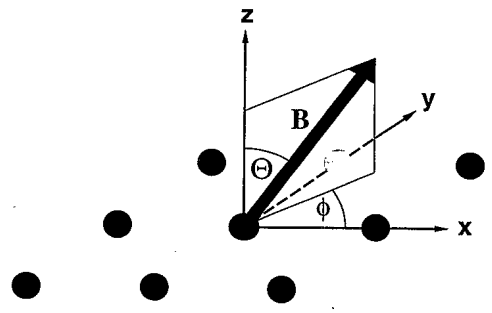

FIG. 1. Magnetic field pointing into a general direction characterized by angles Θ and ϕ, relative to a two-dimensional square lattice.

the axis of $\mathbf{B}$ into the direction $\hat{\mathbf{z}}$. Furthermore, let $\underline{t}(E)$ refer to the single-site $\mathbf{t}$ matrix (matrix representation in angular momentum space) if $\mathbf{B}$ is parallel to the z axis, while $\underline{t}_R(E)$ refers to the $\mathbf{t}$ matrix if $\mathbf{B}$ points along the direction $R^{-1}\hat{\mathbf{z}}$. Because the effective potential and magnetic field are spherical symmetric, these two single-site $\mathbf{t}$-matrices are related to each other by the following similarity transformation:

$$\underline{t}_R(E) = \underline{D}(R)\underline{t}(E)\underline{D}(R)^+\,, \quad (5)$$

where $\underline{D}(R)$ contains blockwise the irreducible projective representations of R.

Relativistic spin-polarized multiple scattering theory was formulated originally by Schadler and co-workers[19,20] and Strange *et al.*[21] A latter rigorous derivation for the more general case of space-filling potentials by Wang *et al.*[36] stresses the formal similarities to the familiar expressions of "standard" multiple scattering theory for muffin-tin potentials.[37] Within multiple scattering theory the Green function, i.e., the configuration space representation of the resolvent $\mathcal{G}(E)$ of the Hamiltonian for an ensemble of individual scatterers is given by

$$\langle \mathbf{r} \mid \mathcal{G}(E) \mid \mathbf{r}' \rangle = \sum_{QQ'} Z_Q^n(E,\mathbf{r}_n)\,\tau_{QQ'}^{nm}(E)\,Z_{Q'}^m(E,\mathbf{r}'_m)^\dagger$$
$$-\delta_{nm}\sum_Q \left\{J_Q^n(E,\mathbf{r}_n)Z_Q^n(E,\mathbf{r}'_n)^\dagger\Theta(\mathrm{r}_n-\mathrm{r}'_n) + Z_Q^n(E,\mathbf{r}_n)J_Q^n(E,\mathbf{r}'_n)^\dagger\Theta(\mathrm{r}'_n-\mathrm{r}_n)\right\}, \quad (6)$$

where n,m label sites, Q,Q' denote pairs of quantum numbers, $Q=(\kappa\mu)$, $\tau_{QQ'}^{nm}$ is the corresponding matrix element of the scattering path operator (SPO), and $\Theta(x)$ denotes the step function. The normalization of the regular and irregular scattering solutions, $Z_Q^n(E,\mathbf{r}_n)$ and $J_Q^n(E,\mathbf{r}_n)$, can be found, e.g., in Ref. 21. It was pointed out by Tamura[38] that the right- and left-hand-side solutions to Diraq equation cannot, in general, be used interchangeably because of the required Herglotz properties in the complex energy plane. However, by evaluating (6) in a local coordinate system, where the magnetic field points along the z axis, one easily can show that the right-hand-side expression can always be used, whereby for any complex energy $z = E+i\delta$, the Hermitean conjugation (†) leaves the radial part of the scattering solutions unchanged.

In order to calculate the SPO's for systems with two-dimensional translational symmetry, we recently developed the screened Korringa-Kohn-Rostoker method (SKKR), which, due to the screened structure constants,[30] makes use of block-tridiagonal supermatrices. By using the corresponding single-site quantities, the relativistic SKKR Green function method[39] can be extended also to spin-polarized systems. In this case, however, special care has to be taken in performing the occurring Brillouin zone integrals needed to evaluate the SPO's, since in the presence of a magnetic field these integrals can no longer be restricted to an irreducible wedge

of the corresponding surface Brillouin zone (SBZ). Let G be the point group of the underlying two-dimensional translational lattice, such as, for example, C_{4v} in the case of an fcc(001) surface, and suppose $\underline{D}(S)$ contains blockwise the irreducible projective representations[40] of $S \in G$. If IBZ_1 denotes an irreducible wedge of the SBZ, then any other wedge IBZ_S of the SBZ is defined by

$$\mathrm{IBZ}_S = \{S\mathbf{k}_\parallel \mid \mathbf{k}_\parallel \in \mathrm{IBZ}_1\}; \quad S \in G, \tag{7}$$

such that

$$\mathrm{SBZ} = \sum_{S \in G} \mathrm{IBZ}_S \ .$$

It easily can be shown that

$$\underline{\tau}^{pq}(S^{-1}\mathbf{k}_\parallel; E) = \underline{D}(S)^{+} \underline{\tau}_S^{pq}(\mathbf{k}_\parallel; E) \underline{D}(S) \ , \tag{8}$$

where p, q are layer indices and the SPO $\underline{\tau}_S^{pq}(\mathbf{k}_\parallel; E)$ refers to the corresponding similarity transformed $\mathbf{t}$ matrix $\underline{t}_S^p(E)$, as defined in Eq. (5). The SBZ integral for the SPO's can therefore be expressed as

$$\underline{\tau}^{pq}(E) = \sum_{S \in G} \underline{D}(S)^{+} \left[\frac{1}{\Omega_{\mathrm{IBZ}_1}} \int_{\mathrm{IBZ}_1} d\mathbf{k}_\parallel \, \underline{\tau}_S^{pq}(\mathbf{k}_\parallel; E) \right] \times \underline{D}(S) \ , \tag{9}$$

where Ω_{IBZ_1} denotes the surface area of IBZ_1. Equation (9) implies (i) that the structure constants need only be evaluated for a chosen set of $\mathbf{k}_\parallel \in \mathrm{IBZ}_1$ and (ii) that for any pair $S, R \in G$ for which $\underline{t}_S^p(E) = \underline{t}_R^p(E)$ the integrals in Eq. (9) are identical. For a magnetic field perpendicular to the surface, for example, the number of integrals to be performed is reduced therefore to 2 (proper and improper rotations).

Based on the Green function (6) physical observables can be evaluated in the usual manner (see, e.g., in Ref. 41). For matters of completeness below, only the corresponding expressions (in units of μ_B) for the spin-only magnetic moments m_{spin} and the orbital magnetic moments m_{orb} are given,

$$m_{\mathrm{spin}} = -\frac{1}{\pi} \mathrm{Im} \int_C dz \ \mathrm{Tr} \{\beta \sigma_z \mathcal{G}(z)\} \ , \tag{10}$$

$$m_{\mathrm{orb}} = -\frac{1}{\pi} \mathrm{Im} \int_C dz \ \mathrm{Tr} \{\beta L_z \mathcal{G}(z)\} \ , \tag{11}$$

where C denotes an integration contour in the upper half of the complex energy plane, which starts at a real energy point below the valence band and ends at the Fermi energy, Tr denotes the trace in the tensorial space of spin and configuration, and L_z is the z component of the angular momentum operator.

III. COMPUTATIONAL DETAILS

Self-consistent calculations within the local spin density approximation (LSDA), the atomic sphere approximation (ASA), and with a magnetic field pointing perpendicular to the surface were carried out in turn for each multilayer system $\mathrm{Fe}_n\mathrm{Au}(001)$, where n denotes the number of Fe layers on top of a Au(001) surface. Similarly to Ref. 30, the screened two-dimensional (2D) structure constants were calculated by using the structure constants of an ideal 3D fcc lattice. Therefore, the subsequent Fe layers were placed into the perfect fcc(001) layer structure of Au, i.e., no lattice strain was taken into account. For this particular setup, in each case, two layers of empty sphere potentials between the perfect vacuum and the surface, as well as at least two layers of Au potentials between the perfect bulk and the Fe film, were treated self-consistently. During the self-consistent procedure, the energy integrations were performed along a semicircular contour using a 16 point Gaussian sampling on an asymmetric (logarithmic) mesh. For the Brillouin zone integrations 45 $\mathbf{k}_\parallel$ points in IBZ_1 have been used. By using a modification of Broyden's second method[42] fairly fast and accurate convergence for the self-consistent potentials and the interface total energy was obtained.

The evaluation of the magnetic anisotropy energy is based on the so-called "force theorem" or frozen potential approximation. Within this approximation, for each system $\mathrm{Fe}_n\mathrm{Au}(001)$, two calculations were performed using the previously determined self-consistent potentials, namely one with the magnetic field perpendicular to the surface ($\perp$), and one with the magnetic field pointing along the x axis of the 2D square lattice ($\parallel$). In these calculations, only the band energies and the magnetic moments were determined with an extremely high accuracy. For that reason, convergency tests have been made using up to 40 energy points along the contour and up to 325 $\mathbf{k}_\parallel$ points in IBZ_1. It turned out that for a given set of $\mathbf{k}_\parallel$ points, 30 energy points were sufficient to obtain an error well below 0.01 meV/Fe for the difference ΔE_b of the band energies,

$$\Delta E_b = E_b^{\parallel} - E_b^{\perp} \ .$$

For a single Fe overlayer on a Au(001) surface, Fig. 2 shows the convergence of ΔE_b with respect to the number of $\mathbf{k}_\parallel$ points in IBZ_1. Due to the enormous computational efforts, for all other cases presented in this paper, we used

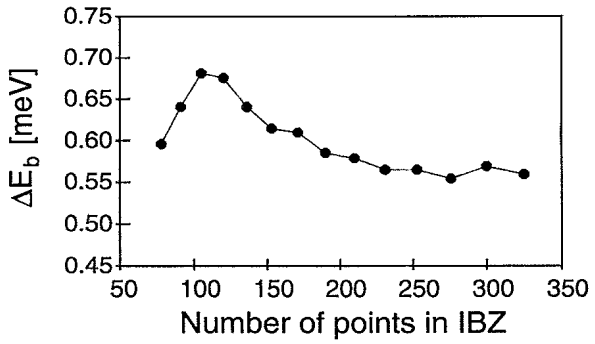

FIG. 2. Convergence of the band energy difference, $\Delta E_b = E_b^{\parallel} - E_b^{\perp}$, for a Fe monolayer on Au(001) with respect to the number of $\mathbf{k}_\parallel$ points in the irreducible wedge of the 2D Brillouin zone. The solid line serves as a guide for the eye.

TABLE I. Calculated spin-only magnetic moments (μ_B) for $Fe_nAu(001)$ multilayers, for a magnetic field pointing along the z axis.

n	Fe(1)	Fe(2)$\cdots$ Fe(n)		Au(1)	Au(2)			
1	3.155	0.006	-0.009					
2	3.071	3.041	0.023	-0.006				
3	3.067	2.974	3.030	0.023	-0.005			
4	3.075	2.950	2.971	3.026	0.022	-0.006		
5	3.071	2.940	2.927	2.947	3.022	0.023	-0.006	
6	3.075	2.949	2.937	2.923	2.964	3.031	0.025	-0.005

210 $\mathbf{k}_{||}$ points, which—as can be seen from Fig. 2—ensure a relative accuracy of about 5% for ΔE_b.

Within the frozen potential approximation the total magnetic anisotropy energy ΔE is then given by the sum of ΔE_b and the anisotropy energy related to the magnetostatic dipole-dipole interaction, ΔE_{dd},

$$\Delta E = \Delta E_b + \Delta E_{dd} \,, \tag{12}$$

which for systems with two-dimensional translational symmetry is discussed in the Appendix.

IV. RESULTS

Let us first discuss the results of the self-consistent calculations corresponding to an orientation of the magnetic field perpendicular to the surface. The layer-resolved spin-only magnetic moments ($m_{\rm spin}$) of the $Fe_nAu(001)$ multilayers are displayed in Table I. As compared to the values calculated recently within a scalar-relativistic layer KKR method by Crampin,[43] using an approximate model for the strained geometry, it is not surprising that in the present case of increased volumes per Fe atoms also the calculated magnetic moments are enhanced. Inspecting Table I, one can see that the spin-only magnetic moments related to the Fe layers show symmetric behavior going from the top of the surface to the Fe layer closest to the first Au layer. This behavior fits well to a similar observation made in Ref. 43 and simply indicates rather weak hybridization between the Fe and Au d bands. It is worthwhile to note that the $m_{\rm spin}$'s for Fe(n) sites, $n \geq 2$, are in very good agreement with those calculated by the spin-polarized relativistic LMTO method[24] for an unstrained Au/Fe/Au(001) interface ($3.046\mu_B$), whereas the $m_{\rm spin}$'s on the Au(1) sites ($\sim 0.023\mu_B$) are closer to the corresponding values in Ref. 43 ($\sim 0.04\ \mu_B$) than to the values given in Ref. 24 ($0.001\mu_B$). This probably is due to the fact that in Ref. 24 an $FeAu_5$ supercell geometry has been used, while in the present method and also in Ref. 43 a true semi-infinite system is considered.

The calculated orbital magnetic moments ($m_{\rm orb}$), see Eq. (11), are shown in Table II. Quite obviously, the top Fe layer again carries the largest moment. It should be noted that for $n \geq 4$ the calculated $m_{\rm orb}$'s for the nth Fe layer and the two subsequent Au layers, Au(1) and Au(2), agree very well with the corresponding values in Ref. 24 ($0.094\mu_B$, $0.015\mu_B$, and $-0.002\mu_B$, respectively).

In Fig. 3 for all the multilayers under consideration the total magnetic anisotropy energy ΔE is shown together with the corresponding band energy contribution ΔE_b and the magnetostatic dipole-dipole interaction energy ΔE_{dd}. The positive values of ΔE_b clearly indicate that spin-orbit coupling favors a perpendicular orientation for the magnetic field. As can be seen, ΔE_b shows quite large fluctuations for a small number of Fe layers, but tends to a value of about 0.6 meV for $n = 5, 6$. These fluctuations are considerably smaller in magnitude than those obtained very recently for ferromagnetic slabs by Cinal *et al.*,[44] using a tight-binding model. In order to explain these fluctuations Cinal *et al.* investigated *partial* anisotropy constants and concluded that beyond the surface layers all layers in the slab had significant contributions to the magnetic anisotropy.[44] Within the multiple scattering theory it is straightforward to split up ΔE_b into contributions related to different layers (Table III). The leading contribution to the anisotropy arises from the Fe layer at the Fe/Au interface, Fe(n). This indeed suggests that the substrate plays an important role for the actual magnitude of surface magnetic anisotropies. With the exception of $n = 2$, the surface Fe layer, Fe(1) also has a large positive contribution to the anisotropy. Quite surprisingly, the Fe layers between these two layers have negative contributions. Nevertheless, these con-

TABLE II. Calculated orbital magnetic moments (μ_B) for $Fe_nAu(001)$ multilayers, for a magnetic field pointing along the z axis.

n	Fe(1)	Fe(2)$\cdots$ Fe(n)		Au(1)	Au(2)			
1	0.125	0.017	-0.002					
2	0.129	0.110	0.015	-0.001				
3	0.125	0.101	0.106	0.017	-0.001			
4	0.113	0.093	0.093	0.093	0.018	-0.001		
5	0.117	0.091	0.095	0.087	0.095	0.018	-0.001	
6	0.115	0.090	0.088	0.085	0.087	0.094	0.018	-0.001

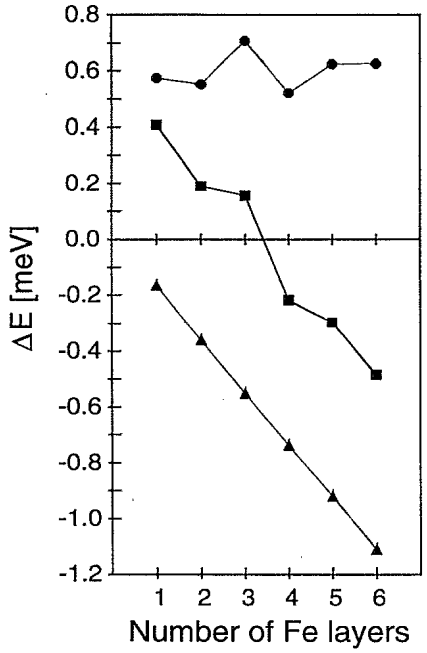

FIG. 3. Calculated magnetic anisotropy energies for Fe multilayers on Au(001). ΔE_b: circles, ΔE_{dd}: triangles, $\Delta E = \Delta E_b + \Delta E_{dd}$: squares. Solid lines serve as a guide for the eye.

tributions tend to decrease rapidly towards the middle of the Fe film. Therefore, the band energy part of the magnetic anisotropy energy for the whole multilayer system converges rapidly with respect to the thickness of the multilayer. It is worthwhile to mention that also the top Au layers remarkably contribute to the magnetic anisotropy energy.

Since the magnetostatic dipole-dipole interaction favors an in-plane orientation of the magnetization, in Fig. 3 ΔE_{dd} is shown with the opposite sign as compared to ΔE_b. Due to the short range nature of the 2D dipole-dipole Madelung constants (see the Appendix), ΔE_{dd} decreases almost linearly with an increasing number of Fe layers. In total, the magnetic anisotropy energy is positive for $n \leq 3$ and negative for $n \geq 4$. The present calculations for $Fe_nAu(001)$ multilayers predict therefore a magnetization perpendicular to the surface up to a multilayer thickness of 3 ML Fe, and an in-plane magnetization beyond that. Despite the oversimplified geometry we used in our calculations (no surface relaxation), the agreement to the "switching" thickness of 2.8 ML found experimentally[28] is excellent.

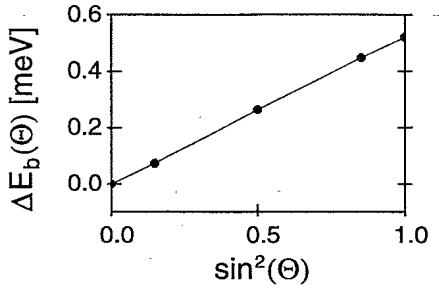

FIG. 4. Dependence of the band energy difference, $\Delta E_b(\Theta) = E_b(\Theta) - E_b^{\perp}$, with respect to the azimuthal angle Θ for the case of 4 Fe ML's on Au(001). The solid line serves as a guide for the eye.

It was shown by Bruno[4] in terms of a tight-binding model and using perturbation theory that for ferromagnetic monolayers (i) the magnetic anisotropy energy is closely related to the anisotropy of the orbital magnetic moment and (ii) for square and hexagonal 2D lattices both are linear functions of $\sin^2(\Theta)$, where Θ is the angle between the normal vector of the plane and the magnetic field (see Fig. 1). These features have then been confirmed by *ab initio* calculations[10–14] even for multilayers, however, treating the spin-orbit coupling as a perturbation to a scalar-relativistic Hamiltonian. Recently, Weller *et al.*[45] reported enhanced orbital moments of Co atoms in Co/Pd and Co/Pt multilayers in connection with strong perpendicular magnetization.

In Table IV the differences of the orbital moments between a perpendicular and an in-plane orientation, $\Delta m_{\rm orb} = m_{\rm orb}^{\parallel} - m_{\rm orb}^{\perp}$, are listed. From this table, one immediately can see a large perpendicular enhancement (negative values) of $m_{\rm orb}$ for the Fe(n) layers. Comparing with Table III, it seems at first glance that this enhancement follows the big anisotropy energy contributions arising from these layers. There is, however, no straightforward proportionality between the anisotropy of the layer-resolved orbital moments and the corresponding anisotropy energies. An obvious deviation from the tight-binding prediction can be seen for the Fe(1) layer in the $n \geq 2$ cases, where an enhancement of $m_{\rm orb}$ for the parallel orientation is found, whereas the corresponding magnetic anisotropy energy contributions are still positive. This implies that the relationship between the orbital moments and magnetic anisotropy energies is much more complicated for multilayer systems as predicted for monolayers from a simple tight-binding model.

As an example for the orientational dependence of

TABLE III. Layer-resolved band energy contributions to the magnetic anisotropy energy (meV), $\Delta E_b = E_b^{\parallel} - E_b^{\perp}$, for $Fe_nAu(001)$ multilayers.

n	Fe(1)	Fe(2)$\cdots$	Fe(n)	Au(1)	Au(2)			
1	0.454	0.160	-0.002					
2	0.034	0.522	0.027	0.015				
3	0.168	-0.117	0.585	0.078	0.025			
4	0.141	-0.088	-0.129	0.514	0.087	0.028		
5	0.204	-0.086	-0.003	-0.123	0.544	0.092	0.021	
6	0.178	-0.031	-0.014	-0.033	-0.088	0.543	0.085	0.021

TABLE IV. Calculated changes of orbital magnetic moments ($10^{-3}\mu_B$), $\Delta m_{\rm orb} = m^{\parallel}_{\rm orb} - m^{\perp}_{\rm orb}$, for $Fe_nAu(001)$ multilayers.

n	Fe(1)	Fe(2)$\cdots$	Fe(n)	Au(1)	Au(2)			
1	-29.1	2.9	1.3					
2	5.1	-37.3	6.3	1.2				
3	8.3	-7.9	-30.2	2.9	0.9			
4	7.3	0.3	-1.3	-23.3	1.7	1.2		
5	4.3	0.2	-5.7	2.1	-25.2	2.5	1.1	
6	3.6	0.5	-2.2	3.7	-0.3	-26.3	2.4	0.7

ΔE_b, calculations have been carried out for $Fe_4Au(001)$ for $\Theta = \pi/8, \pi/4$, and $3\pi/8$. As can be seen from Fig. 4, the corresponding results for ΔE_b are almost perfectly linear with $\sin^2(\Theta)$. Similarly, the orbital moments exhibit also a nearly linear dependence on $\sin^2(\Theta)$, i.e., higher order terms [$\sin^4(\Theta)$, etc.] could not be established within the accuracy of our calculations. Additional calculations with $\phi = \pi/8$ and $\pi/4$ proved that within an accuracy of much less than 0.01 meV, ΔE_b is independent of ϕ. Recalling Eq. (A9), it can be concluded that for the present system the total magnetic anisotropy energy is proportional to $\sin^2(\Theta)$, i.e., is monotonously increasing for $n \leq 3$ and monotonously decreasing for $n \geq 4$ as a function of Θ. At least for the ground state (T=0), this implies that for up to 3 ML Fe on Au(001) only a perpendicular orientation of the magnetization is stable, while for more than 3 ML an in-plane orientation of the magnetization is favored.

ACKNOWLEDGMENTS

The authors are grateful for stimulating discussions with B. L. Györffy, R. Monnier, and H. Dreyssé. This paper was supported by the Austrian Ministry of Science (GZ 45.368/2-IV/6/94 and GZ 45.340/2-IV/6a/94) and the Austrian National Bank (P4648). Two of us (L.S. and B.U.) are also indebted to the Hungarian National Scientific Research Foundation for partial financial support (OTKA-517/1990 and OTKA F014378).

APPENDIX A: THE MAGNETOSTATIC DIPOLE-DIPOLE INTERACTION FOR FERROMAGNETIC LAYERED SYSTEMS

If one partitions the configurational space into cells centered around positions $\mathbf{R}$, then within the dipole approximation the relativistic current-current interaction energy is reduced to the magnetostatic dipole-dipole interaction energy, which can be expressed in atomic Rydberg units as[46]

$$E_{dd} = \frac{1}{c^2} {\sum_{\mathbf{R},\mathbf{R}'}}' \left\{ \frac{\mathbf{m_R} \mathbf{m_{R'}}}{|\mathbf{R}-\mathbf{R}'|^3} - 3 \frac{[\mathbf{m_R}\cdot(\mathbf{R}-\mathbf{R}')][\mathbf{m_{R'}}\cdot(\mathbf{R}-\mathbf{R}')]}{|\mathbf{R}-\mathbf{R}'|^5} \right\} , \tag{A1}$$

where $\mathbf{m_R}$ is the magnetic moment at site $\mathbf{R}$ and the prime at the summation indicates a restriction to $\mathbf{R} \neq \mathbf{R}'$. Since we are dealing with ferromagnetic systems, i.e.,

$$\mathbf{m_R} = m_{\mathbf{R}}\, \hat{\mathbf{n}} ,$$

and since two-dimensional (2D) translational invariance pertains within the layers,

$$\mathbf{R} = \mathbf{R}_{p\alpha} + \mathbf{R}_{\parallel} ,$$

where $\mathbf{R}_{\parallel}$ denotes a 2D real lattice vector and $\mathbf{R}_{p\alpha}$ specifies a site in the unit cell of the system at layer p and sublattice α, Eq. (A1) can be rewritten as

$$E_{dd} = \sum_{p\alpha,q\beta} \frac{m_{p\alpha} m_{q\beta}}{c^2}\, \hat{\mathbf{n}}\, \underline{M}^{dd}_{p\alpha,q\beta}\, \hat{\mathbf{n}} . \tag{A2}$$

In (A2) the so-called 2D ferromagnetic dipole-dipole Madelung constant matrix is defined by

$$\underline{M}^{dd}_{p\alpha,q\beta} = {\sum_{\mathbf{R}_{\parallel}}}' \frac{1}{|\mathbf{R}_{p\alpha}-\mathbf{R}_{q\beta}-\mathbf{R}_{\parallel}|^3} \left\{ \underline{I} - \frac{(\mathbf{R}_{p\alpha}-\mathbf{R}_{q\beta}-\mathbf{R}_{\parallel}) \otimes (\mathbf{R}_{p\alpha}-\mathbf{R}_{q\beta}-\mathbf{R}_{\parallel})}{|\mathbf{R}_{p\alpha}-\mathbf{R}_{q\beta}-\mathbf{R}_{\parallel}|^2} \right\} , \tag{A3}$$

where $\underline{I}$ is a 3×3 unit matrix and $\otimes$ denotes a tensorial product of vectors. In (A3) the prime indicates that for $\mathbf{R}_{p\alpha}=\mathbf{R}_{q\beta}$ the singular term corresponding to $\mathbf{R}_{\parallel}=0$ is excluded from the summation.

TABLE V. Ferromagnetic dipole-dipole Madelung constants, M_{pq}^{dd}, for fcc(001) planes in units of $1/a^3$, where a denotes the 2D lattice constant.

$p-q$	0	1	2	3
M_{pq}^{dd}	9.033 62	1.429 41	-0.022 64	0.000 26

For $|\mathbf{R}_{p\alpha;\perp}-\mathbf{R}_{q\beta;\perp}| \neq 0$ the magnetostatic Poisson equation can be solved in a straightforward manner (see also Ref. 47). Similarly to the electrostatic case it is possible to use a Fourier expansion[48] that results in a fast convergent series

$$\underline{M}_{p\alpha,q\beta}^{dd} = -\frac{2\pi}{A}\sum_{\mathbf{G}_\parallel\neq 0} |\mathbf{G}_\parallel| \exp\left(-|\mathbf{G}_\parallel||\mathbf{R}_{p\alpha;\perp}-\mathbf{R}_{q\beta;\perp}|\right)\exp\left(i\,\mathbf{G}_\parallel\cdot(\mathbf{R}_{p\alpha;\parallel}-\mathbf{R}_{q\beta;\parallel})\right) \times \begin{pmatrix} -\frac{\mathbf{G}_\parallel\otimes\mathbf{G}_\parallel}{|\mathbf{G}_\parallel|^2} & -i\,\mathrm{sgn}\,(\mathbf{R}_{p\alpha;\perp}-\mathbf{R}_{q\beta;\perp})\,\frac{\mathbf{G}_\parallel\otimes 1}{|\mathbf{G}_\parallel|} \\ -i\,\mathrm{sgn}\,(\mathbf{R}_{p\alpha;\perp}-\mathbf{R}_{q\beta;\perp})\,\frac{1\otimes\mathbf{G}_\parallel}{|\mathbf{G}_\parallel|} & 1 \end{pmatrix}, \tag{A4}$$

where A is the 2D unit cell area and $\mathbf{G}_\parallel$ is a 2D reciprocal space vector. It should be noted that the $\mathbf{G}_\parallel=0$ component does not contribute to the "off-plane" terms. For the (001) and (111) faces of the simple cubic lattices (sc, bcc, or fcc), (A4) can be further reduced to

$$\underline{M}_{pq}^{dd} = M_{pq}^{dd} \times \begin{pmatrix} -\frac{1}{2} & 0 & 0 \\ 0 & -\frac{1}{2} & 0 \\ 0 & 0 & 1 \end{pmatrix}, \tag{A5}$$

where

$$M_{pq}^{dd} = -\frac{2\pi}{A}\sum_{\mathbf{G}_\parallel\neq 0} |\mathbf{G}_\parallel| \exp\left(-|\mathbf{G}_\parallel|\,|\mathbf{R}_{p;\perp}-\mathbf{R}_{q;\perp}|\right)\,\cos\left[\mathbf{G}_\parallel\cdot(\mathbf{R}_{p;\parallel}-\mathbf{R}_{q;\parallel})\right]. \tag{A6}$$

Restricting ourselves to this special case, the 2D ferromagnetic dipole-dipole Madelung constants for $p=q$ can be evaluated by using a standard Ewald summation technique to give

$$M_{pp}^{dd} = \sum_{\mathbf{R}_\parallel\neq 0}\left\{\frac{\mathrm{erfc}\left(|\mathbf{R}_\parallel|/2\sigma\right)}{|\mathbf{R}_\parallel|^3} + \frac{\exp\left(-|\mathbf{R}_\parallel|^2/4\sigma^2\right)}{\sigma\sqrt{\pi}\,|\mathbf{R}_\parallel|^2}\right\} -\frac{2\pi}{A}\sum_{\mathbf{G}_\parallel\neq 0}\left\{|\mathbf{G}_\parallel|\,\mathrm{erfc}\left(|\mathbf{G}_\parallel|\sigma\right) - \frac{1}{\sigma\sqrt{\pi}}\exp\left(-|\mathbf{G}_\parallel|^2\sigma^2\right)\right\} - \frac{1}{6\sigma^3\sqrt{\pi}} + \frac{2\sqrt{\pi}}{A\sigma}, \tag{A7}$$

where σ is the Ewald parameter and $\mathrm{erfc}(x)=1-\mathrm{erf}(x)$.[49] The independence of (A7) from the Ewald parameter has been tested numerically for a wide range of σ. Table V clearly indicates the fast decay of the magnetic dipole-dipole interaction with the distance between layers. For practical purposes contributions to magnetic anisotropy energy from next nearest neighbor planes and beyond can be neglected.

Finally, the orientational dependence of the magnetostatic dipole-dipole energy shall be discussed. By using the usual expression of the unit vector $\hat{\mathbf{n}}=[\sin(\Theta)\cos(\phi), \sin(\Theta)\sin(\phi), \cos(\Theta)]$, one immediately obtains that

$$\hat{\mathbf{n}}\begin{pmatrix} -\frac{1}{2} & 0 & 0 \\ 0 & -\frac{1}{2} & 0 \\ 0 & 0 & 1 \end{pmatrix}\hat{\mathbf{n}} = \frac{3}{2}\cos^2(\Theta) - \frac{1}{2}, \tag{A8}$$

which implies that the orientational dependence of the magnetostatic dipole-dipole anisotropy energy, ΔE_{dd}, can be simply written as[47]

$$\Delta E_{dd}(\Theta) = (E_{dd}^{\parallel} - E_{dd}^{\perp})\,\sin^2(\Theta). \tag{A9}$$

[1] L.M. Falicov, D.T. Pierce, S.D. Bader, R. Gronsky, K.B. Hathaway, H.J. Hopster, D.N. Lambeth, S.P. Parkin, G. Prinz, M. Salamon, I.K. Schuller, and R.H. Victora, J. Mater. Res. **5**, 1299 (1990).
[2] S.D. Bader, Proc. IEEE **78**, 909 (1990).
[3] J.H. van Vleck, Phys. Rev. **52**, 1178 (1937).
[4] P. Bruno, Phys. Rev. B **39**, 865 (1989).
[5] Š. Pick and H. Dreyssé, Phys. Rev. B **46**, 5802 (1992).
[6] Š. Pick, J. Dorantes-Dávila, G.M. Pastor, and H. Dreyssé, Phys. Rev. B **50**, 993 (1994).
[7] J.G. Gay and R. Richter, Phys. Rev. Lett. **56**, 2728 (1986).
[8] J.G. Gay and R. Richter, J. Appl. Phys. **61**, 3362 (1987).
[9] C. Li, A.J. Freeman, H.J.F. Jansen, and C.L. Fu, Phys. Rev. B **42**, 5433 (1990).
[10] G.H.O. Daalderop, P.J. Kelly, and M.F.H. Schuurmans, Phys. Rev. B **42**, 7270 (1990).

[11] G.H.O. Daalderop, P.J. Kelly, and M.F.H. Schuurmans, Phys. Rev. B **44**, 12 054 (1992).
[12] G.H.O. Daalderop, P.J. Kelly, and F.J.A. den Broeder, Phys. Rev. Lett. **68**, 682 (1992).
[13] D.S. Wang, R. Wu, and A.J. Freeman, Phys. Rev. Lett. **70**, 869 (1993).
[14] D.S. Wang, R. Wu, and A.J. Freeman, Phys. Rev. B **47**, 14 932 (1993).
[15] R.H. Victora and J.M. MacLaren, Phys. Rev. B **47**, 11 583 (1993).
[16] E.M. Rose, *Relativistic Electron Theory* (Wiley, New York, 1971).
[17] R. Feder and F. Rosicky, Z. Phys. B **52**, 52 (1983).
[18] P. Strange, J. Staunton, and B.L. Györffy, J. Phys. C **17**, 3355 (1984).
[19] G. Schadler, P. Weinberger, A.M. Boring, and R.C. Albers, Phys. Rev. B **34**, 713 (1986).
[20] G. Schadler, R.C. Albers, A.M. Boring, and P. Weinberger, Phys. Rev. B **35**, 4324 (1987).
[21] P. Strange, H. Ebert, J. Staunton, and B.L. Györffy, J. Phys. Condens. Matter **1**, 2959 (1989).
[22] H. Ebert, P. Strange, and B.L. Györffy, J. Appl. Phys. **63**, 3052 (1988).
[23] H. Ebert, Phys. Rev. B **38**, 9390 (1988).
[24] G.Y. Guo, W.M. Temmerman, and H. Ebert, J. Phys. Condens. Matter **3**, 8205 (1991).
[25] G.Y. Guo, W.M. Temmerman, and H. Ebert, J. Magn. Magn. Mater. **104-107**, 1772 (1992).
[26] D. Bader and E.R. Moog, J. Appl. Phys. **61**, 3729 (1987).
[27] R. Germar, W. Dürr, J.W. Krewer, D. Pescia, and W. Gudat, Appl. Phys. A **47**, 393 (1988).
[28] C. Liu and S.D. Bader, J. Vac. Sci. Technol. A **8**, 2727 (1990).
[29] A.M. Begley, S.K. Kim, J. Quinn, F. Jona, H. Over, and P.M. Marcus, Phys. Rev. B **48**, 1779 (1993).
[30] L. Szunyogh, B. Újfalussy, P. Weinberger, and J. Kollár, Phys. Rev. B **49**, 2721 (1994).
[31] A.K. Rajagopal, J. Phys. C **11**, L943 (1978).
[32] A.H. MacDonald and S.H. Vosko, J. Phys. C **12**, 2977 (1979).
[33] G. Baym, *Lectures on Quantum Mechanics* (Benjamin, New York, 1969).
[34] A.C. Jenkins and P. Strange, J. Phys. Condens. Matter **6**, 3499 (1994).
[35] S.C. Lovatt, B.L. Györffy, and G.Y. Guo, J. Phys. Condens. Matter **5**, 8005 (1993).
[36] X. Wang, X.-G. Zhang, W.H. Butler, G.M. Stocks, and B.N. Harmon, Phys. Rev. B **46**, 9352 (1992).
[37] J.S. Faulkner and G.M. Stocks, Phys. Rev. B **21**, 3222 (1980).
[38] E. Tamura, Phys. Rev. B **45**, 3271 (1992).
[39] L. Szunyogh, B. Újfalussy, P. Weinberger, and J. Kollár, J. Phys. Condens. Matter **6**, 3301 (1994).
[40] S.L. Altmann and P. Herzig, *Point-Group Theory Tables* (Clarendon, Oxford, 1994).
[41] P. Weinberger, *Electron Scattering Theory for Ordered and Disordered Matter* (Clarendon, Oxford, 1990).
[42] D.D. Johnson, Phys. Rev. B **38**, 12 807 (1988)
[43] S. Crampin, J. Phys. Condens. Matter **5**, 4647 (1993).
[44] M. Cinal, D.M. Edwards, and J. Mathon, Phys. Rev. B **50**, 3754 (1994).
[45] D. Weller, Y. Wu, J. Stöhr, M.G. Samant, B.D. Hermsmeier, and C. Chappert, Phys. Rev. B **49**, 12 888 (1994).
[46] G.H.O. Daalderop, P.J. Kelly, M.F.H. Schuurmans, and F. Jansen, Phys. Rev. B **41**, 11 919 (1990).
[47] E. Tsymbal, J. Magn. Magn. Mater. **130**, L6 (1994).
[48] J.M. MacLaren, S. Crampin, D.D. Vvedensky, and J.B. Pendry, Phys. Rev. B **40**, 12 164 (1989).
[49] *Handbook of Mathematical Functions*, edited by M. Abramowitz and I.A. Stegun (Dover, New York, 1970).